


 Cite this: *New J. Chem.*, 2020, **44**, 129

# Highly active mesoionic chalcogenone zinc(II) derivatives for C–S cross-coupling reactions†

 Moulali Vaddamanu,<sup>a</sup> Kavitha Velappan<sup>b</sup> and Ganesan Prabusankar<sup>ib</sup>\*<sup>a</sup>

The first mesoionic heavier chalcogenones, **L**<sup>1</sup>–**L**<sup>3</sup> [**L**<sup>1</sup> = 1-(2-mesitylene)-3-methyl-4-phenyltriazolin-5-selone; **L**<sup>2</sup> = 1-(2-mesitylene)-3-methyl-4-phenyltriazolin-5-thione; **L**<sup>3</sup> = 1-(benzyl)-2-3(methyl)-4-phenyltriazolin-5-selone], were isolated and characterised. Density functional theory was used to obtain insights into the  $\sigma$  donor and  $\pi$  accepting nature of mesoionic chalcogenones. Using these new ligands, a series of the first zinc(II) mesoionic chalcogenone complexes were isolated. Three mono nuclear zinc(II) chalcogenone complexes, [(**L**<sup>1</sup>)Zn(Cl)<sub>2</sub>(HOMe)] (**1**), [(**L**<sup>2</sup>)Zn(Cl)<sub>2</sub>(HOMe)] (**3**) and [(**L**<sup>3</sup>)Zn(Br)<sub>2</sub>(HOMe)] (**4**), and two dinuclear zinc complexes, [(**L**<sup>1</sup>)Zn(Br)( $\mu^2$ -Br)]<sub>2</sub> (**2**) and [(**L**<sup>3</sup>)Zn(Br)( $\mu^2$ -Br)]<sub>2</sub> (**5**), containing mesoionic thione and selone ligands were synthesized and characterised. These new complexes **1**–**5** represent the first structurally characterized mesoionic chalcogenone supported metal derivatives. Furthermore, all zinc complexes were characterized by thermogravimetric analysis and UV-vis spectroscopy. The solid-state structures of all zinc complexes were determined by single-crystal X-ray diffraction. The catalytic activities of the zinc(II) complexes in thioetherification reactions were investigated without scrubbing of oxygen. The scope of the catalytic reactions was explored with a wide range of thiophenols and aryl halides. The diaryl thioethers were obtained in very good yield under mild conditions. The present protocol furnishes a synthetic route for the C–S cross-coupling of thiophenols and aryl halides without scrubbing oxygen and moisture.

 Received 27th August 2019,  
 Accepted 19th November 2019

DOI: 10.1039/c9nj04440j

rsc.li/njc

## Introduction

The application of mesoionic carbene (MIC) or “abnormal” N-heterocyclic carbene (*a*NHC) supported metal derivatives has continued to expand at a rapid rate in catalysis compared to N-heterocyclic carbene (NHC) metal derivatives.<sup>1–4</sup> The better  $\sigma$  donor and poor  $\pi$  accepting nature of MICs along with low steric hindrance compared to NHCs provide greater control on the metal centers for improved catalytic performance.<sup>7–9</sup> The first MIC carbenes and their transition metal derivatives were reported by Crabtree and co-workers.<sup>10</sup> Subsequently, several MIC–metal complexes have subsequently been reported with potential roles in synthetic and catalytic applications.<sup>1–9</sup> Though the MICs and related chemistry have been known for a while, the triazolylidene type of MIC chemistry is relatively new. The triazolylidene family of MICs was discovered by

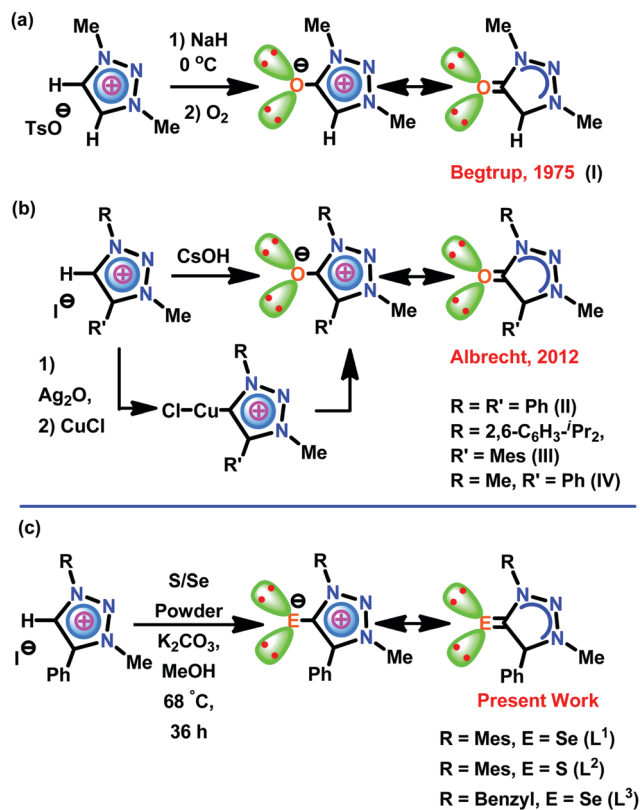
Begtrup *et al.* in 1975.<sup>11</sup> Begtrup isolated the first mesoionic oxide (**I**) through short-lived 1*H*-1,2,3-triazol-5-ylidene by deprotonation of the triazolium salt with NaH at 0 °C in the presence of oxygen (Scheme 1a).<sup>11</sup> Later Enders used triazolylidenes as organocatalysts in 1995.<sup>12</sup> Albrecht reported the synthesis of 1,2,3-triazolylidenes using a Huisgen cycloaddition between azides and alkynes in 2008.<sup>13</sup> Thus the first 1,2,3-triazolylidene based MIC-Pd/Ag/Rh/Ir molecules were reported.<sup>13</sup> Later, Bertrand succeeded in isolating and characterizing the first free triazolylidene.<sup>14</sup> Notably, the triazole framework is versatile for introducing substituents and electronically unique as the carbenic carbon in triazolylidenes is flanked by only one heteroatom.<sup>15</sup> The most recent review by Bertrand summarizes the advancement of triazolylidene chemistry.<sup>9</sup>

Though Begtrup accounted for the first mesoionic oxide (**I**) *via* short-lived 1*H*-1,2,3-triazol-5-ylidene, thirty-seven years later, Albrecht reported the first solid-state structure of mesoionic oxide **II–IV** (Scheme 1b).<sup>16a</sup> **II–IV** were derived *via* the reaction between Cu(I) triazolylidenes or triazolium salts and CsOH. Also, the *in situ* generation of **II**-CuCl was used as a catalyst in [3+2] dipolar cycloaddition of alkynes and azides (a ‘click’ reaction). Notably, the catalytic efficiency of **II**-CuCl was comparable with the corresponding copper(I) 1,2,3-triazol-5-ylidene complex.<sup>16b,c</sup> However, the heavier congeners of 1,2,3-triazole based mesoionic chalcogenone have not been isolated yet.

<sup>a</sup> Department of Chemistry, Indian Institute of Technology Hyderabad, Kandi, TS, 502285, India. E-mail: prabu@iith.ac.in; Fax: +914023016032; Tel: +914023016089

<sup>b</sup> Department of Chemistry, GITAM University, Hyderabad, TS, 502329, India

† Electronic supplementary information (ESI) available: <sup>1</sup>H and <sup>13</sup>C NMR spectra of the synthesized complexes. Solid state packing. Computational data. CCDC 1893235 (**L**<sup>1</sup>), 1893237 (**L**<sup>2</sup>), 1893236 (**L**<sup>3</sup>), 1893242 (**1**), 1893241 (**2**), 1893240 (**3**), 1893238 (**4**), 1893239 (**5**) and 1895992 (**E14**). For ESI and crystallographic data in CIF or other electronic format see DOI: 10.1039/c9nj04440j



Scheme 1 Synthesis of mesoionic chalcogenones.

However, despite the growing number of examples documenting imidazole chalcogenone (IMC) chemical reactivity, over the last ten years, IMCs have proven to be pivotal supporting ligands for a variety of catalytically active metal complexes. We also noted the seminal contribution of Nolan, Son, Sing, and others, who have reported a broad range of imidazole chalcogenones (IMCs), such as imidazole thione (IMT) and imidazole selone (IMSe). The IMC Pd(II), Ir(III), Au(I), Au(III), Cu(I), Zn(II), Cd(II), Bi(III), Ni(II), Ru(II) and Rh(III) derivatives were used as catalysts in the Heck coupling reaction,<sup>17</sup> Suzuki–Miyaura coupling,<sup>18</sup> Sonogashira coupling,<sup>18b</sup> oxidative coupling of benzylamine to imine under visible-light,<sup>19</sup> regioselective borylation of internal alkynes,<sup>20,21</sup> hydroamination reactions,<sup>22,23</sup> click chemistry,<sup>23,24</sup> nitroarene reduction to aromatic amines,<sup>25</sup> Barbier reactions in aqueous media,<sup>26</sup> *o*-acylative cleavage of cyclic ethers,<sup>27</sup> triarylmethane synthesis,<sup>28</sup> norbornene polymerization,<sup>29</sup> oxidation of alcohols,<sup>30</sup> catalytic transfer hydrogenation reactions,<sup>31–33</sup> *N*-alkylation of anilines,<sup>33</sup> and cross-dehydrogenative coupling of alkynes with silanes.<sup>24</sup> In most cases, the catalytic efficiency of IMC–metal complexes is comparable or even much more efficient compared to the corresponding metal–NHC derivatives.<sup>20,23,24</sup>

In contrast, the literature reveals a dearth of studies about the chemistry of mesoionic chalcogenone (MIC) metal complexes. Thus, we believe that the heavier mesoionic type of triazole chalcogenone (TAC) complexes are expected to have great potential for the evolution of new catalysts with unprecedented ligand-induced catalytic control. On the basis of this evolution,

herein, we report the first examples of heavier mesoionic chalcogenones,  $L^1$ – $L^3$  [ $L^1$  = 1-(2-mesitylene)-3-methyl-4-phenyl-triazolin-5-selone;  $L^2$  = 1-(2-mesitylene)-3-methyl-4-phenyl-triazolin-5-thione;  $L^3$  = 1-(benzyl)-2-(3-methyl)-4-phenyl-triazolin-5-selone], through a one-pot synthesis. Besides,  $L^1$ – $L^3$  were used as ligands in isolating the mononuclear zinc(II) metal complexes  $[(L^1)Zn(Cl)_2(HOMe)]$  (1),  $[(L^2)Zn(Cl)_2(HOMe)]$  (3), and  $[(L^2)Zn(Br)_2(HOMe)]$  (4) and dinuclear zinc(II) metal complexes  $[(L^1)Zn(Br)(\mu^2-Br)]_2$  (2), and  $[(L^3)Zn(Br)(\mu^2-Br)]_2$  (5). Subsequently, 1–5 were used as catalysts for C–S cross-coupling reactions between thiophenols and aryl halides. These catalytic reactions can be carried out at 80 °C and less reaction time without scrubbing of oxygen, comprising a substantial advantage over known  $ZnEt_2$ -mediated cross-coupling reactions.

## Results and discussion

Recently we have performed a comparative study between  $Ph_3P$ , NHC, and IMC supported copper(I) complexes for C–N and C–Si bond formation reactions.<sup>24</sup> Based on the  $\sigma$ -donor and  $\pi$ -accepting strength, we assumed that  $[(IMes=S)Cu]$  [ $IMes=S=1,3$ -bis(2,4,6-trimethylphenyl)imidazolin-2-thione] was more active than  $[(IMes)CuCl]$  [ $IMes=1,3$ -bis(2,4,6-trimethylphenyl)imidazol-2-ylidene] for the synthesis of 1,2,3-triazoles and for the cross-dehydrogenative coupling of alkynes with silanes. However, the  $\sigma$ -donor and  $\pi$ -accepting nature of NHCs vs. IMCs remains unclear. In particular, the chemistry of the mesoionic type of heavier chalcogenones has never been investigated. Therefore Density Functional Theory (DFT) calculations were carried out at the B3LYP level using an all-electron basis set which includes polarization and diffuse functions (6-311++G\*\*) for 1,3,4-trimethyl-1,2,3-triazolin-5-ylidene (I), 1,3,4-trimethyl-1,2,3-triazolin-5-thione (II) and 1,3,4-trimethyl-1,2,3-triazolin-5-selone (III) to understand the  $\sigma$ -donor and  $\pi$ -accepting nature (Fig. 1). Notably, the HOMO energy of II and III is considerably higher than that of I, while the LUMO energy of II and III is lower than that of I. Thus, mesoionic or abnormal NHC analogs II and III can become a good  $\sigma$ -donor and  $\pi$ -acceptor ligand compared to NHC. As a result, II or III can be considered as a potential option to compete with the catalytic properties of mesoionic or abnormal NHC metal derivatives.

The triazolium salts were prepared *via* a copper(I)-catalyzed azide–alkyne cycloaddition reaction followed by methylation of the triazole at the N3-position.<sup>16</sup> The direct thionation or selenation of *N*-alkylated-1,3 disubstituted 1,2,3 triazolium iodides with elemental sulfur or selenium powder in the presence of potassium carbonate gave corresponding mesoionic chalcogenone ligands  $L^1$ ,  $L^2$  and  $L^3$  in excellent yield.<sup>34,35</sup>  $L^1$ ,  $L^2$ , and  $L^3$  are soluble in common nonpolar solvents and mid-polar solvents. These compounds were characterized by FT-IR, UV-vis, and multinuclear NMR techniques. In  $^1H$  NMR, the formation of the chalcogenone derivatives ( $L^1$ ,  $L^2$ , and  $L^3$ ) was supported by the disappearance of an acidic triazolium proton ( $\delta_{H(\text{range})}$  9.52 ppm).<sup>16</sup> In  $^{13}C$  NMR, the chemical shift value of the carbon attached to the chalcogenone in  $L^1$  or  $L^3$  is

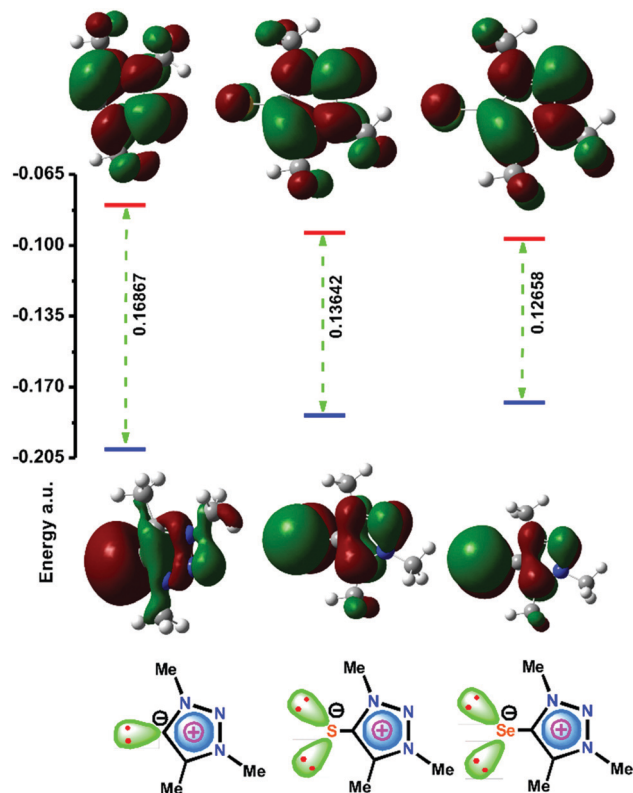


Fig. 1 The comparison of the HOMO and LUMO energy differences between 1,3,4-trimethyl-1,2,3-triazolin-5-ylidene (I), 1,3,4-trimethyl-1,2,3-triazolin-5-thione (II) and 1,3,4-trimethyl-1,2,3-triazolin-5-selone (III). Density Functional Theory (DFT) calculations were carried out at the B3LYP level using an all electron basis set which includes polarization and diffuse functions (6-311++G\*\*).

about 10 ppm upfield shifted compared to  $L^2$ . The  $^{13}\text{C}$  NMR chemical shift value of the carbon attached to the chalcogenone in  $L^1$  or  $L^2$  is comparable with that of IMesSe (IMesSe = 1,3-dimesitylimidazole-2-selone).<sup>28</sup> The solid-state structures of  $L^1$ ,  $L^2$ , and  $L^3$  were determined by single-crystal X-ray diffraction analysis. The molecular structures of  $L^1$ ,  $L^2$ , and  $L^3$  are depicted in Fig. 2.  $L^1$ ,  $L^2$ , and  $L^3$  are the first structurally characterized mesoionic NHC analogs of 1,2,3-triazolin-5-chalcogenones. The C=S bond distance found in  $L^2$  (1.687(2) Å) is 0.017 Å longer than that of IPrS (1.670(3) Å) (IPrS = 1,3-bis(2,6-diisopropylphenyl)imidazole-2-thione).<sup>28</sup> The C=Se bond distance found in  $L^1$  (1.840(4) Å) and  $L^3$  (1.841(5) Å) is marginally longer than that of IMesSe (1.827(6) Å) (IMesSe = 1,3-dimesitylimidazole-2-selone).<sup>28</sup> The C(2)–C(1)–N(1) bond angles found in  $L^1$ ,  $L^2$ , and  $L^3$  are comparable. The C(2)–C(1)–N(1) bond angles found in  $L^1$ ,  $L^2$  and  $L^3$  are comparable to that of IPrS (104.6(2)°) and IMesSe (104.8(5)°).<sup>28</sup> Like 1,2,3-triazolin-5-ylidene,<sup>9</sup> the N–N or C–N or C–C bond distances in  $L^1$ ,  $L^2$ , and  $L^3$  are nearly comparable, which supports the aromatic nature of 1,2,3-triazolin-5-chalcogenones.

The coordination capabilities of these new ligands were investigated with zinc halides in toluene (Schemes 2 and 3).  $L^1$  or  $L^2$  was treated with zinc(II) dihalides followed by recrystallization from a mixed solvent of methanol and chloroform to

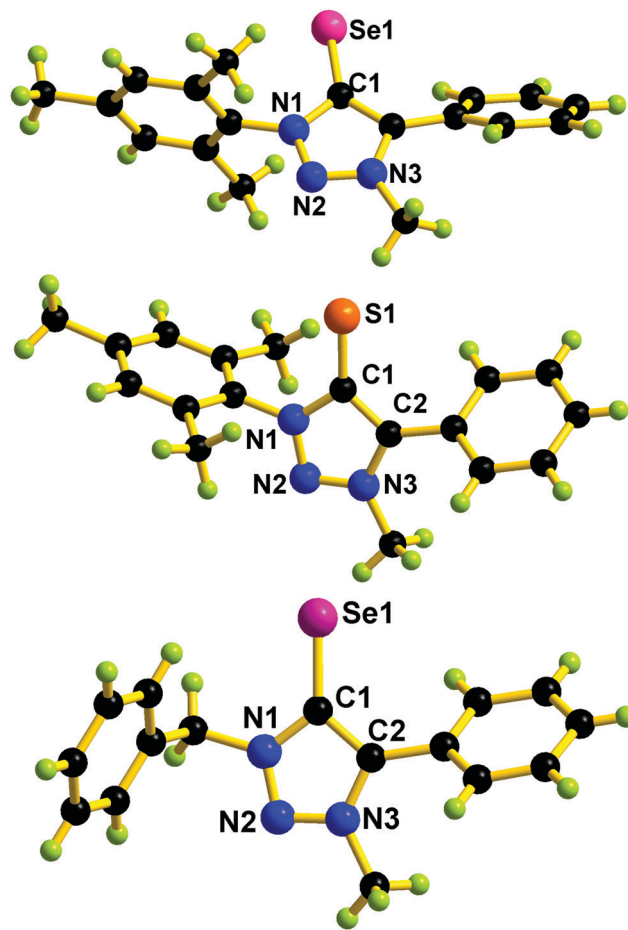
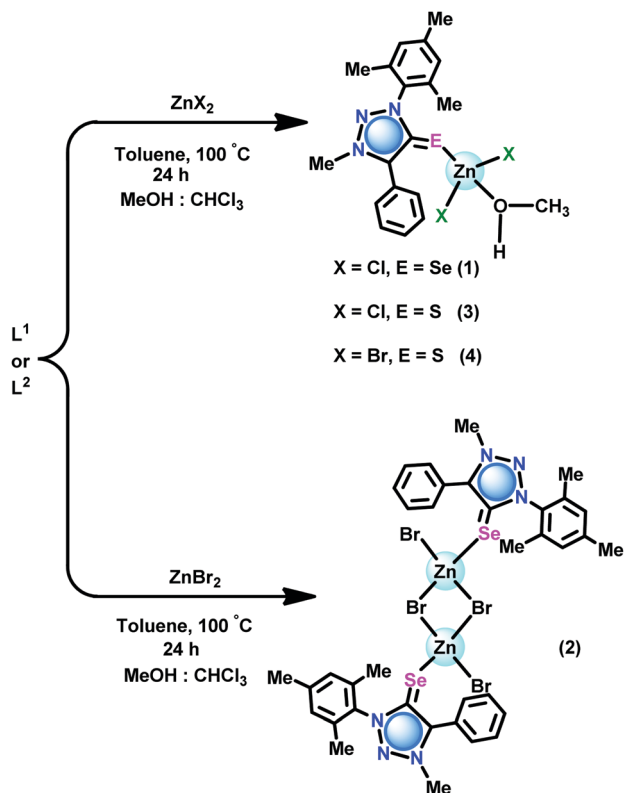


Fig. 2 Top: Molecular structure of  $L^1$ . Selected bond lengths (Å) and bond angles (°): C(1)–Se(1) 1.840(4), N(1)–C(1) 1.377(5), N(3)–C(2) 1.365(5), C(1)–C(2) 1.404(5), N(1)–N(2) 1.338(4), N(2)–N(3) 1.328(5), N(1)–N(2)–N(3) 103.20(3), C(2)–C(1)–N(1) 103.30(3). Middle: Molecular structure of  $L^2$ . Selected bond lengths (Å) and bond angles (°): C(1)–S(1) 1.687(2), N(1)–C(1) 1.385(3), N(3)–C(2) 1.359(3), C(1)–C(2) 1.400(3), N(1)–N(2) 1.339(2), N(2)–N(3) 1.324(3), N(1)–N(2)–N(3) 103.43(17), C(2)–C(1)–N(1) 102.9(2). Bottom: Molecular structure of  $L^3$ . Selected bond lengths (Å) and bond angles (°): C(1)–Se(1) 1.841(4), N(1)–C(1) 1.361(6), N(3)–C(2) 1.360(5), C(1)–C(2) 1.415(7), N(1)–N(2) 1.325(5), N(2)–N(3) 1.307(6), N(1)–N(2)–N(3) 103.50(4), C(2)–C(1)–N(1) 105.8(4).

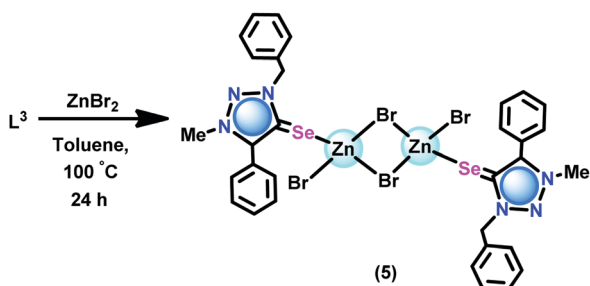
isolate the mono nuclear zinc(II) chalcogenone complexes  $[(L^1)\text{Zn}(\text{Cl})_2(\text{HOME})]$  (1),  $[(L^2)\text{Zn}(\text{Cl})_2(\text{HOME})]$  (3) and  $[(L^3)\text{Zn}(\text{Br})_2(\text{HOME})]$  (4). Under similar reaction conditions, the reaction between  $\text{ZnBr}_2$  and  $L^1$  or  $L^3$  gave dinuclear zinc complexes  $[(L^1)\text{Zn}(\text{Br})(\mu^2\text{-Br})_2]$  (2) and  $[(L^3)\text{Zn}(\text{Br})(\mu^2\text{-Br})_2]$  (5), respectively.

The mesoionic chalcogenone supported zinc complexes (1–5) were characterized by FT-IR, UV-vis, TGA, and multinuclear NMR studies and X-ray diffraction techniques. In the FT-IR spectra, the  $\bar{\nu}_{\text{C}=\text{E}}$  stretching frequency for 1–5 appeared at a 50  $\text{cm}^{-1}$  lower wavenumber (1122–1126  $\text{cm}^{-1}$ ) compared to the corresponding uncoordinated mesoionic thione ligand,  $L^2$  (1173  $\text{cm}^{-1}$ ), or uncoordinated mesoionic selone ligand ( $L^1$  and  $L^3$ ) (1160–1170  $\text{cm}^{-1}$ ).

$L^1$ ,  $L^2$ , and  $L^3$  and 1–5 show an absorption band around 310 nm and 370 nm (Fig. 3, see the ESI†). The UV-vis absorption



Scheme 2 Synthesis of 1–4.



Scheme 3 Synthesis of 5.

pattern of 1–5 is comparable with that of  $\text{L}^1$ ,  $\text{L}^2$ , and  $\text{L}^3$ . The absorption band observed around 310 nm could be attributed to the electron transition associated with  $\pi$  to  $\pi^*$ . The absorption band at 370 nm can be attributed to the  $n$  to  $\pi^*$  transitions. 1 shows both hyperchromic and bathochromic shifts compared to free ligand  $\text{L}^1$ . 3 and 4 depict a hypochromic shift compared to free ligand  $\text{L}^2$ . Besides, the 310 nm zone absorption bands of 3 and 4 show a bathochromic shift compared to free ligand  $\text{L}^2$ . The dinuclear zinc(II) complex 2 shows a hypochromic shift compared to  $\text{L}^1$ , while 5 exhibits a hyperchromic shift compared to  $\text{L}^3$ . Based on the molar extinction coefficient, it is clear that the good  $\sigma$  donor capacity of the mesoionic chalcogenone was noticed with  $\text{Zn(II)Cl}_2$  compared to  $\text{Zn(II)Br}_2$ .

The thermal stability of 1–5 was analyzed by TGA. Fig. 4 presents the amount and rate of change in the weight of the material as a function of temperature (10 °C per minute) under

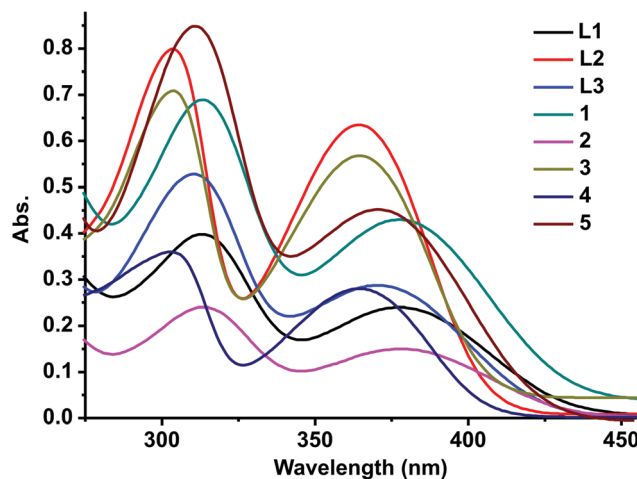
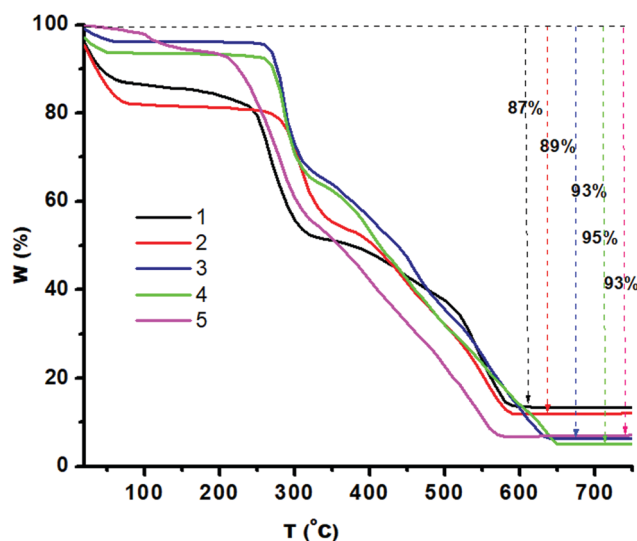
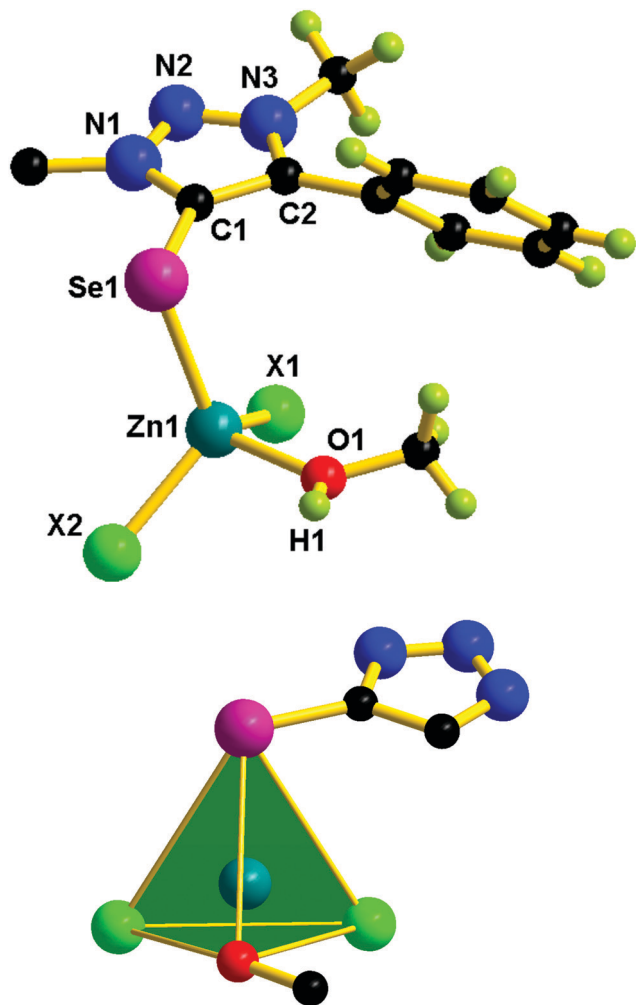
Fig. 3 Solution-state UV-vis spectra of  $\text{L}^1$ ,  $\text{L}^2$ , and  $\text{L}^3$  and 1–5 in DMSO at RT ( $1.04 \times 10^{-4}$  M).

Fig. 4 The thermal stability of compounds 1–5 (10 °C per minute) under a nitrogen atmosphere.

a nitrogen atmosphere. 1, 3 and 4 showed two steps of weight loss due to loss of methanol in step 1 till 100 °C then the organic moiety in step 2 till 500 °C. 5 shows gradual weight loss till 225 °C (8% weight loss) and then gradual weight loss till 560 °C (85% weight loss) due to the loss of organic moieties, while 2 shows three-step weight loss to yield the residue. The unchanged residue of 1–5 must be the corresponding zinc chalcogenides.

The solid-state structures of 1–5 were confirmed by single-crystal X-ray diffraction studies. X-ray quality crystals were isolated from a chloroform and methanol mixture for 1–4, while from toluene for 5. The molecular structures of 1–5 are reported in Fig. 5–7. The crystallographic data for 1–5 are listed in Table S1 (see the ESI<sup>†</sup>). Molecules 1, 3, and 4 are mononuclear zinc(II) complexes, while 2 and 5 are dinuclear zinc(II) complexes. 1, 3, and 4 are isostructural molecules; thus, the



**Fig. 5** Molecular structures of **1**, **3** and **4**. The N(1) substituent is omitted for clarity. Selected bond lengths (Å) and bond angles (°) of **1**: C(1)–Se(1) 1.879(4), Zn(1)–Se(1) 2.436(6), Zn(1)–Cl(1) 2.209(11), Zn(1)–Cl(2) 2.253(13), Zn(1)–O(1) 2.032(3), N(1)–N(2) 1.339(4), N(2)–N(3) 1.320(4), Se(1)–Zn(1)–Cl(1) 95.78(10), Se(1)–Zn(1)–Cl(2) 113.64(4), Se(1)–Zn(1)–O(1) 108.45(10), N(1)–N(2)–N(3) 103.00(3). Selected bond lengths (Å) and bond angles (°) of **3**: C(1)–S(1) 1.719(3), Zn(1)–S(1) 2.326(9), Zn(1)–Cl(1) 2.209(10), Zn(1)–Cl(2) 2.250(9), Zn(1)–O(1) 2.029(3), N(1)–N(2) 1.334(3), N(2)–N(3) 1.318(4), S(1)–Zn(1)–Cl(1) 112.46(3), S(1)–Zn(1)–Cl(2) 113.44(4), S(1)–Zn(1)–O(1) 108.96(10), N(1)–N(2)–N(3) 103.40(2). Selected bond lengths (Å) and bond angles (°) for **4**: C(1)–S(1) 1.717(6), Zn(1)–S(1) 2.326(18), Zn(1)–Br(1) 2.383(11), Zn(1)–Br(2) 2.341(9), Zn(1)–O(1) 2.029(4), N(1)–N(2) 1.342(6), N(2)–N(3) 1.328(6), S(1)–Zn(1)–Br(1) 113.94(5), S(1)–Zn(1)–Br(2) 112.85(5), S(1)–Zn(1)–O(1) 109.10(2), N(1)–N(2)–N(3) 102.50(4).

structural features of **1**, **3**, and **4** are discussed collectively. The Zn(II) center in **1**, **3** and **4** is tetra coordinated by one chalcogenone ligand and two halides and a methanol molecule. The geometry of the zinc(II) center in **1**, **3**, and **4** can be described as tetrahedral. The sums of angles around the zinc(II) center in **1**, **3**, and **4** are comparable. The Zn–Se bond distance found in **1** (2.436(6) Å) is 0.042 Å shorter than that of dichlorobis[1,3-dimethyl-2(3*H*)-imidazole-selone]zinc(II) (2.469 and 2.487 Å)<sup>36</sup> and perchlorate tetra-1-(2,6-diisopropylphenyl)-3-(2-methoxy-2-oxoethyl)-imidazoline zinc(II) (2.463(6) Å).<sup>26</sup> Similarly, the Zn–S bond distance found in **3** (2.326(9) Å) and **4** (2.326(18) Å) is

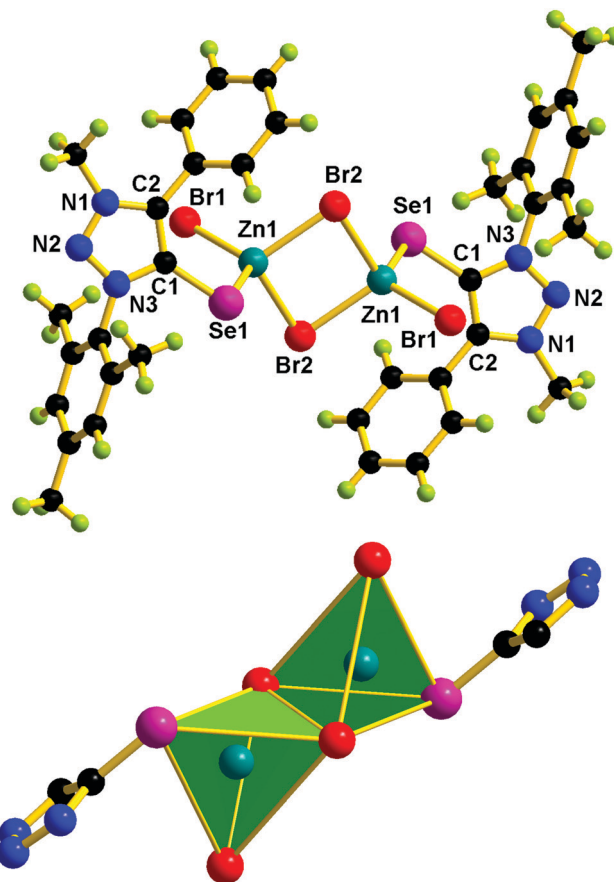


**Fig. 6** Molecular structure of **2**. Selected bond lengths (Å) and bond angles (°): C(1)–Se(1) 1.884(5), Zn(1)–Se(1) 2.416(8), Zn(1)–Br(1) 2.509(9), Zn(1)–Br(2) 2.343(9), N(1)–N(2) 1.320(6), N(2)–N(3) 1.344(5), C(1)–Se(1)–Zn(1) 99.33(15), Br(2)–Zn(1)–Se(1) 103.31(3), Br(1)–Zn(1)–Br(2) 114.84(4), N(1)–N(2)–N(3) 103.20(4).

~0.042 Å shorter than that of dichloridobis(1,3-diisopropyl-4,5-dimethyl-2*H*-imidazole-2-thione)zinc(II) (2.366(9) and 2.370(10) Å).<sup>37</sup>

Molecules **2** and **5** consist of a dinuclear zinc(II) selone core. The core of **2** and **5** is composed of [Zn<sub>2</sub>(Br)<sub>2</sub>(μ<sup>2</sup>-Br)<sub>2</sub>(Se)<sub>2</sub>]. The coordination environment around the zinc center is satisfied by three bromide ions and one selone ligand, which leads to a tetrahedral geometry. Two tetrahedrons are fused through the Br–Br edge to result in the core [Zn<sub>2</sub>(Br)<sub>2</sub>(μ<sup>2</sup>-Br)<sub>2</sub>(Se)<sub>2</sub>].

The bond length and bond angle parameters of **2** and **5** are not comparable. The Zn–Se bond distance in **2** is 0.012 Å shorter than that of **5**. The bridging Zn–Br bond distances in **2** are considerably shorter than the terminal Zn–Br bond distances, while in **5** the terminal Zn–Br bond distances are considerably shorter than the bridging Zn–Br bond distances. The C–Se–Zn bond angle in **2** is slightly wider than that of **5**. The Br–Zn–Br angles in **2** are much wider than those of **5**. The N–N, N–C and C–C bond distances within the five-membered heterocyclic ring are nearly comparable, which supports the existence of resonances within the ring system.

#### Catalyst 1–5 mediated C–S bond formation reactions

Thioethers are important motifs found in organic synthesis, biological chemistry, and materials science. The synthesis of

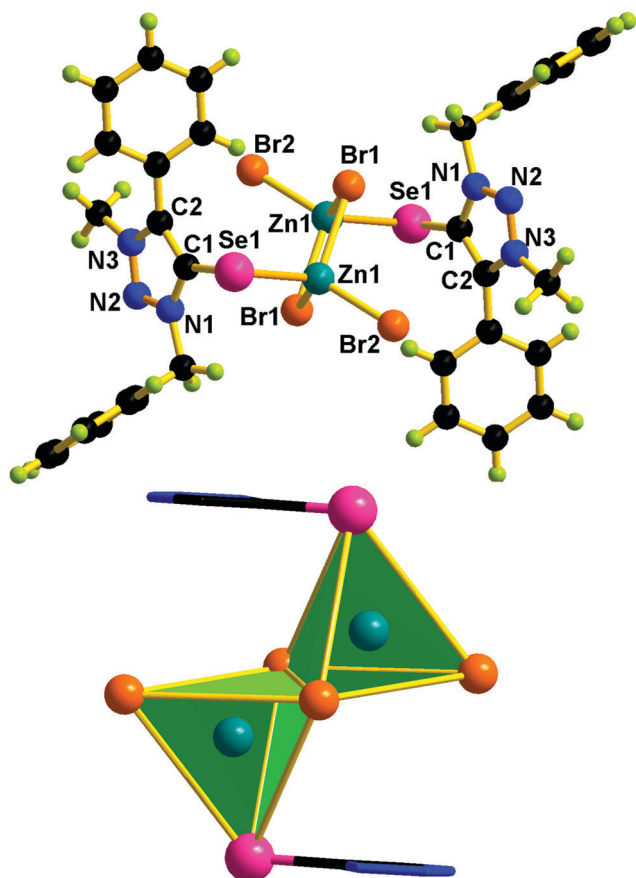
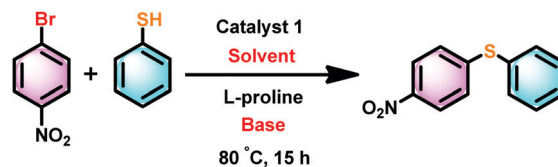


Fig. 7 Molecular structure of **5**. Selected bond lengths (Å) and bond angles (°): C(1)–Se(1) 1.881(5), Zn(1)–Se(1) 2.428(9), Zn(1)–Br(2) 2.498(8), Zn(1)–Br(1) 2.500(9), Zn(1)–Br(1) 2.347(7), N(1)–N(2) 1.315(5), N(2)–N(3) 1.319(5), C(1)–Se(1)–Zn(1) 97.56(15), Br(2)–Zn(1)–Se(1) 108.74(3), Br(1)–Zn(1)–Br(2) 111.20(3), N(1)–N(2)–N(3) 103.50(4).

thioethers can be achieved through cross-coupling of thiophenols and aryl halides using Pd(II), Cu(I), Cu(II), Ir(I), Ni(II), Fe(III), Mn(II), Co(II), In(III), Au(I), Rh(I), Ag(I), Bi(III) and La(III).<sup>38–46</sup> Recently, the C–S coupling protocol was made attractive from an economic standpoint with the use of Et<sub>2</sub>Zn under anaerobic conditions as an alternative to expensive methods.<sup>39a,46</sup> Notably Zn(II) based catalysts for cross-coupling of thiophenols and aryl halides under aerobic conditions are not known.<sup>39–46</sup> Thus molecules **1–5** were used as catalysts to investigate the cross-coupling of thiophenols and aryl halides under aerobic conditions. For example, we have screened catalyst **1** with different bases and solvents at different temperatures to optimize the coupling reaction.

The cross-coupling reaction between 1-bromo-4-nitro benzene and thiophenol was investigated with selected solvents and bases using catalyst **1** as a model system (Scheme 4). Polar to mid-polar solvents such as toluene, MeCN, and THF and bases such as K<sub>2</sub>CO<sub>3</sub>, Cs<sub>2</sub>CO<sub>3</sub>, and <sup>t</sup>BuONa were screened (Fig. 8). The catalytic reactions in solvents toluene and THF were not fruitful. Similarly, bases K<sub>2</sub>CO<sub>3</sub> and Cs<sub>2</sub>CO<sub>3</sub> were not suitable for the catalytic conversion. The control reactions using only ZnX<sub>2</sub> or ZnX<sub>2</sub>·6H<sub>2</sub>O with NaOtBu (2 equiv.) in MeCN were unsuccessful,



Scheme 4 Optimization of the solvent and base for the catalyst **1** mediated cross-coupling reaction between 1-bromo-4-nitro benzene and thiophenol.

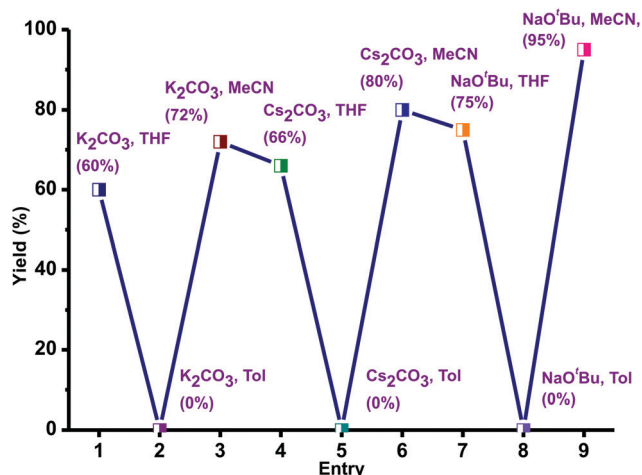
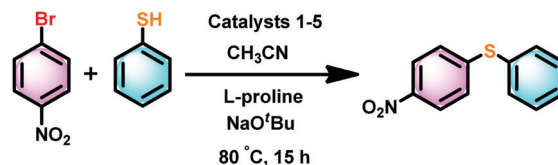


Fig. 8 Optimization of the solvent and bases in catalyst **1** mediated thioetherification of aryl halides. Reaction conditions: 1-bromo-4-nitro benzene (1 mmol), thiophenol (1 mmol), base (2 equiv.), catalyst **1** (10 mol%), L-proline (10 mol%), 80 °C, 15 h.

while ZnBr<sub>2</sub> with NaOtBu (2 equiv.) in MeCN gave a poor yield (for more information see the ESI,† Tables S5 and S6).<sup>46</sup> The best results were obtained in acetonitrile and NaO<sup>t</sup>Bu at 80 °C within 15 h. Thus, the desired product was isolated and conveniently separated by column chromatography.

The cross-coupling reaction between 1-bromo-4-nitro benzene and thiophenol can also be catalyzed by ZnCl<sub>2</sub> or ZnBr<sub>2</sub> or strong bases.<sup>46</sup> However, the isolated yield was very poor (5% to 25%) under very high catalyst loading with a high temperature in more than 24 h.

To compare the catalytic efficiency of **1–5**, catalytic reactions were carried out between 1-bromo-4-nitrobenzene and thiophenol using the zinc catalyst (10 mol%) and L-proline (10 mol%) (Scheme 5). Catalysts **1–5** are very active and yielded the corresponding thioether in excellent yield within 15 h (Fig. 9). Among catalysts **1–5**, catalyst **1** is found to be very active. As reported,<sup>39,46</sup>



Scheme 5 Catalyst **1–5** mediated cross-coupling reaction between 1-bromo-4-nitro benzene and thiophenol.

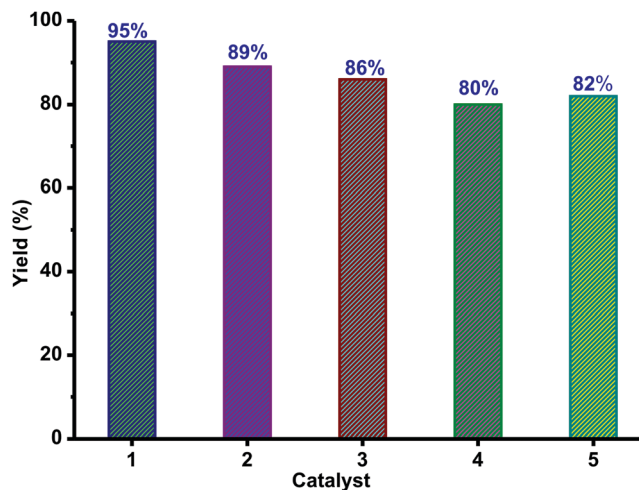


Fig. 9 The catalyst **1–5** mediated cross-coupling reaction between 1-bromo-4-nitro benzene and thiophenol. Reaction conditions: 1-bromo-4-nitro benzene (1 mmol), thiophenol (1 mmol), NaO<sup>t</sup>Bu (2 equiv.), catalyst (10 mol%), L-proline (10 mol%), 80 °C, 15 h.

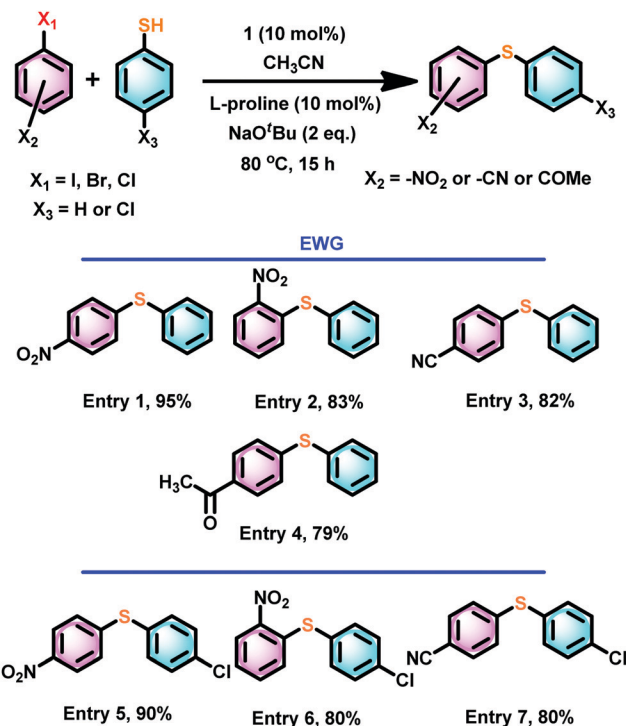
more than 50% of known catalysts were used in 10% catalyst loading, while up to 20% catalyst loading has been utilized in most cases. Therefore, the catalyst loading in the present report is well within the reported range for C–S cross-coupling reactions. This is essential to decrease the reaction time (for more information see the ESI,† Table S6).

Thus, we have assessed the scope of catalyst **1** with a different combination of electron-deficient aryl halides or thiophenols (Scheme 6). The cross-coupling reactions between thiophenol and 1-halo-EWG-benzene (EWG = 4-NO<sub>2</sub> (entry 1), 2-NO<sub>2</sub> (entry 2), 4-CN (entry 3), 4-COMe (entry 4)) gave excellent yields. Similarly, excellent cross-coupling conversion was achieved between 4-chloro thiophenol and 4-nitro/2-nitro/4-cyano aryl halide (Scheme 6, entries 5–7)

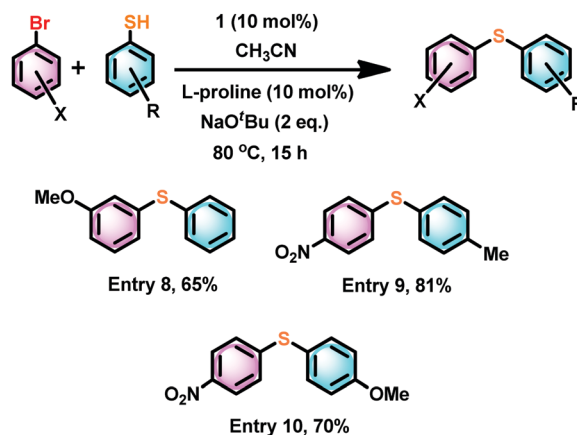
The coupling reaction between an aryl halide such as 1-bromo-3-methoxy-benzene and thiophenol under the same conditions gave about 30% less yield compared to much more electron-deficient aryl halides (Scheme 7, entry 8). However, the combination of both 4-nitro-1-bromo benzene and 4-methyl and 4-methoxy aryl thiol gave a very good yield (Scheme 7, entries 9 and 10).

Similarly, the cross-coupling reaction between 2-bromo-3-nitropyridine and 4-methoxy thiophenol gave a cross-coupled product with good yield (Scheme 8). Hence, the electron-rich aryl halides are compatible with these conditions to yield cross-coupled products in excellent yield.

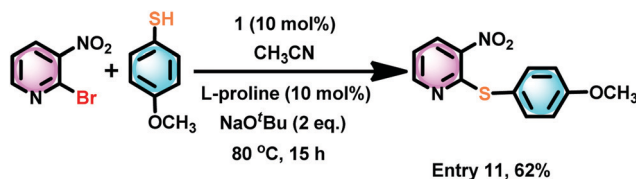
2-(Arylthio)benzothiazoles are considered to be a potential class of bioactive ingredients in the pharmaceutical industry.<sup>47</sup> Thus, the catalytic efficiency of **1** was investigated for the thioetherification between 2-mercaptobenzothiazole and 4-nitro thiophenol (Scheme 9). 2-(4-Nitrophenylthio)benzothiazole was isolated in excellent yield (86%). The catalyst **1** mediated synthesis of 2-(4-nitrophenylthio)benzothiazole appears to be more efficient than the CuBr mediated tandem one-pot synthesis at 80 °C for 15 h (70%),<sup>48</sup> the FeCl<sub>3</sub>–N,N'-dimethylethylenediamine mediated



Scheme 6 Scope of catalyst **1** mediated thioetherification of electron withdrawing group substituted aryl halides.

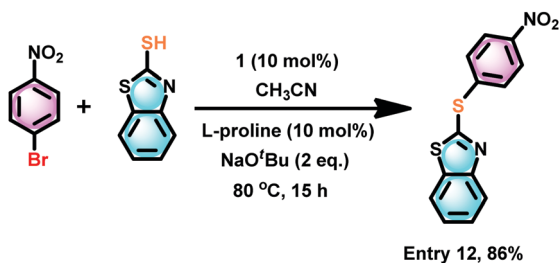


Scheme 7 The influence of an electron-rich aryl halide or aryl thiol in catalyst **1** mediated thioetherification reactions.



Scheme 8 The catalyst **1** mediated thioetherification reaction between 2-bromo-3-nitropyridine and 4-methoxy thiophenol.

reaction at 135 °C for 24 h (83%),<sup>49</sup> enaminone ligand assisted copper(II)-catalyzed at 100 °C for 12 h (51%),<sup>50</sup> and copper(I)-catalyzed at 100 °C for 24 h (83%).<sup>51</sup>



Scheme 9 The catalyst **1** mediated thioetherification of 2-mercapto-benzothiazole with an electron withdrawing group substituted aryl halide, such as 4-nitro thiophenol.

Also, we have attempted to isolate polyaromatic scaffolds, such as anthracene thioether derivatives. Similar molecules have shown promising features in anti-counterfeiting technology,<sup>52</sup> medicinal chemistry,<sup>53</sup> and the electronics industry as soft materials,<sup>54</sup> to name a few. Under the above-optimized reaction conditions with catalyst **1**, the C–S cross-coupling strategy was explored with 9-bromo anthracene. The C–S bond formation reaction between 9-bromo anthracene and 4-halo aryl thiols in the presence of catalyst **1** gave 9-(4-halo phenylthio)-anthracene in very good yield (74–70%) (Scheme 10, entries 13–15). It is noteworthy that the 9-(4-fluoro phenylthio)-anthracene, 9-(4-chloro phenylthio)-anthracene and 9-(4-bromo phenylthio)-anthracene derivatives have never been isolated. The present strategy results the formation of these rare molecules in pure form. The solid-state structure of 9-(4-chloro phenylthio)-anthracene has been characterised by the single-crystal X-ray diffraction technique (Fig. 10). The C(9)–S(1) and C(3)–S(1) bond distances are nearly comparable. The C(9)–S(1)–C(3) angle is 102.16(7)°. In the molecular packing of 9-(4-chloro phenylthio)-anthracene, pairs of 9-(4-chloro phenylthio)-anthracene molecules are arranged orthogonal to each other without any van der Waals interaction (see the ESI<sup>†</sup>). The present protocol seems to be competitive enough with the recently developed most efficient C–S cross-coupling reaction to isolate an unfunctionalized

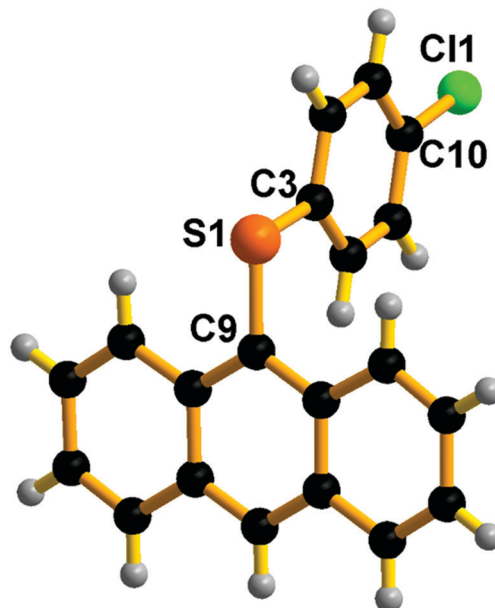


Fig. 10 Molecular structure of **E14**. Selected bond lengths (Å) and bond angles (°): C(3)–S(1) 1.770(17), C(9)–S(1) 1.776(17), C(9)–S(1)–C(3) 102.16(7).

9-(phenylthio)-anthracene using an air and moisture stable bimetallic catalyst  $[(t\text{-Bu}_3\text{P})\text{Pd}(\text{I})_2]$ , 89%).<sup>55</sup>

Besides, the isolated yield under the above synthetic methodology is more commodious and economical under mild reaction conditions compared to the known methodologies.<sup>39</sup>

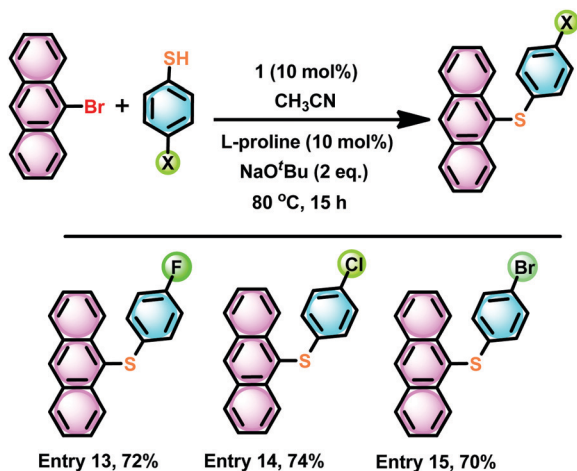
It is important to note that the addition of *L*-proline is very much essential to activate the catalyst. The catalyst is inactive in the absence of *L*-proline or the presence of less than 10 mol% *L*-proline. Furthermore, the blank reaction under optimized conditions gave zero progress in the catalytic conversion. Besides, the reaction mechanism and scope of the metal choice are yet to be explored further. Currently, we are working in this direction.

## Experimental section

### Materials and methods

All manipulations were carried out under an argon atmosphere using standard Schlenk techniques. The solvents were purchased from commercial sources and purified according to standard procedures and freshly distilled under an argon atmosphere before use. Phenyl acetylene, methyl iodide, sulfur powder, selenium powder, zinc chloride, and zinc bromide were purchased from commercial sources. Aromatic azides,  $\text{CuBr}(\text{PPh}_3)_3$ , 1-mesityl-3-methyl-4-phenyl-1*H*-1,2,3-triazol-3-ium iodide, and 1-benzyl-3-methyl-4-phenyl-1*H*-1,2,3-triazol-3-ium iodide, were prepared as described in the literature.<sup>13,16</sup>

**Caution!** Organic azides and sodium azide are potentially-explosive substances. Azide salts tend to be highly heat and shock-sensitive explosives. Avoid strong acids, which can lead to the formation of hydrazoic acid, which is highly toxic, volatile, and explosive. Handle sodium azide powder or solutions > 5%



Scheme 10 The catalyst **1** mediated thioetherification of 4-halo thiophenol with anthracene bromide.

only in a properly functioning fume hood. Wear respiratory protection. Wear personal protective equipment. Avoid dust formation. Do not get in the eyes, or on the skin, or clothing. Use only under a chemical fume hood. Do not breathe vapors/dust. Do not ingest.

FT-IR measurements (neat) were carried out on a Bruker Alpha-P Fourier transform spectrometer. The UV-vis spectra were recorded on a T90+UV-vis spectrophotometer. The thermogravimetric analysis (TGA) was performed using a TASCOT Q600. The NMR spectra were recorded on Bruker Ultrashield-400 spectrometers at 25 °C unless otherwise stated. Chemical shifts are given relative to TMS and were referenced to the solvent resonances as internal standards. Single crystals of complexes suitable for single-crystal X-ray analysis were obtained from their reaction mixture in a chloroform and methanol mixture (1:1 ratio) at room temperature. Suitable crystals of **L**<sup>1</sup>–**L**<sup>3</sup>, **1**–**5** and **E14** were selected and mounted on a SuperNova, Dual, Cu at zero, Eos diffractometer. The crystal was kept at 298 K during data collection. Using Olex2,<sup>56</sup> the structure was solved with the olex2.solve<sup>57</sup> structure solution program using direct methods and refined with the olex2.refine<sup>58</sup> refinement package using Gauss–Newton minimization. Absorption corrections were performed based on multiple scans. Non-hydrogen atoms were anisotropically refined. Hydrogen atoms were included in the refinement in the calculated positions riding on their carrier atoms. **L**<sup>1</sup> and **L**<sup>3</sup> gave one “A” level alert due to a negligible difference in the measured fraction theta full value (0.861 for **L**<sup>1</sup> and 0.925 for **L**<sup>3</sup>). Attempts to rectify these issues were not fruitful. Molecule **5** gave one “B” level alert due to the disordered carbon atoms of the benzene/toluene molecule. Though the reaction was carried out and crystallized in toluene, the lattice solvent molecule in **5** was fixed as benzene due to the heavily disordered nature of the lattice solvent molecule. Our efforts to locate the toluene methyl group were not successful. However the disordered lattice solvent molecule in **5** has no implication for the structural properties of metal complex **5**.

#### Synthesis of 1-mesityl-3-methyl-4-phenyl-1,2,3-triazole selone (**L**<sup>1</sup>)

To dry potassium carbonate (1.36 g, 9.87 mmol), 1-mesityl-3-methyl-4-phenyl-1*H*-1,2,3-triazol-3-ium iodide (1.6 g, 3.95 mmol), Se powder (0.4 g, 5.19 mmol) and methanol (20 mL) were added under an argon atmosphere. The reaction mixture was stirred for 36 h at 68 °C. The progress of the reaction was monitored by TLC. After completion of the reaction, water was added to the reaction mixture and extracted with dichloromethane (3 × 15 mL). The organic extract was washed with brine solution, and dried over anhydrous Na<sub>2</sub>SO<sub>4</sub>. The organic solvent was evaporated under reduced pressure to isolate analytically pure **L**<sup>1</sup>. Yield: 77% (based on the triazolium salt). M.p.: 190–195 °C. <sup>1</sup>H NMR (CDCl<sub>3</sub>, 400 MHz): δ 7.82 (d, *J* = 7.4 Hz, 2H, *H*<sub>Ar</sub>), 7.52 (m, 3H, *H*<sub>Ar</sub>), 7.03 (s, 2H, *H*<sub>Mes</sub>), 4.16 (s, 3H, N-CH<sub>3</sub>), 2.36 (s, 3H, Ar-CH<sub>3</sub>), 2.09 (s, 6H, Ar-CH<sub>3</sub>). <sup>13</sup>C NMR (CDCl<sub>3</sub>, 100 MHz): δ 148.95 (C=Se), 141.42 (C<sub>trz</sub>-Mes), 140.67 (C<sub>trz</sub>-Ph), 135.28 (C<sub>Ar</sub>), 132.81 (C<sub>Ar</sub>), 130.13 (C<sub>Ar</sub>), 129.25 (C<sub>Ar</sub>), 128.92 (C<sub>Ar</sub>), 126.06 (C<sub>Ar</sub>), 38.62 (N-CH<sub>3</sub>), 21.32 (Ar-CH<sub>3</sub>), 18.09 (Ar-CH<sub>3</sub>). FT-IR (neat,  $\bar{\nu}$ ): 2920(m), 2855(w), 1600(m),

1523(w), 1445(s), 1319(w), 1285(w), 1170(s) (C=Se), 1113(m), 1069(s), 1020(m), 855(s), 763(m), 693(s), 539(s) cm<sup>-1</sup>.

#### Synthesis of 1-mesityl-3-methyl-4-phenyl-1,2,3-triazole thione (**L**<sup>2</sup>)

**L**<sup>2</sup> was prepared by a procedure analogous to that of **L**<sup>1</sup> starting from 1-mesityl-3-methyl-4-phenyl-1*H*-1,2,3-triazol-3-ium iodide (1.6 g, 3.95 mmol) and sulfur powder (0.25 g, 7.36 mmol). Yield: 80% (based on the triazolium salt). M.p.: 170–175 °C. <sup>1</sup>H NMR (CDCl<sub>3</sub>, 400 MHz): δ 7.81 (d, *J* = 8.12 Hz, 2H, *H*<sub>Ar</sub>), 7.49 (m, 3H, *H*<sub>Ar</sub>), 7.02 (s, 2H, *H*<sub>Mes</sub>), 4.11 (s, 3H, N-CH<sub>3</sub>), 2.34 (s, 3H, Ar-CH<sub>3</sub>), 2.11 (s, 6H, Ar-CH<sub>3</sub>). <sup>13</sup>C NMR (CDCl<sub>3</sub>, 100 MHz): δ 158.76 (C=S), 140.55 (C<sub>trz</sub>-Mes), 137.10 (C<sub>trz</sub>-Ph), 135.55 (C<sub>Ar</sub>), 131.94 (C<sub>Ar</sub>), 129.76 (C<sub>Ar</sub>), 129.26 (C<sub>Ar</sub>), 128.91 (C<sub>Ar</sub>), 126.12 (C<sub>Ar</sub>), 38.80 (N-CH<sub>3</sub>), 21.30 (Ar-CH<sub>3</sub>), 17.96 (Ar-CH<sub>3</sub>). FT-IR (neat,  $\bar{\nu}$ ): 2915(w), 2853(w), 1602(m), 1523(w), 1461(s), 1400(w), 1336(s), 1286(m), 1173(s) (C=Se), 1116(m), 1063(m), 1020(s), 861(s), 797(m), 759(s), 697(s), 546(s) cm<sup>-1</sup>.

#### Synthesis of 1-benzyl-3-methyl-4-phenyl-1,2,3-triazole selone (**L**<sup>3</sup>)

**L**<sup>3</sup> was prepared by a procedure analogous to that of **L**<sup>1</sup> starting from 1-benzyl-3-methyl-4-phenyl-1*H*-1,2,3-triazol-3-ium iodide (1.5 g, 3.97 mmol) and selenium powder (0.31 g, 3.97 mmol). Yield: 84% (based on the triazolium salt). M.p.: 152–155 °C. <sup>1</sup>H NMR (DMSO-*d*<sub>6</sub>, 400 MHz): δ 7.64 (m, 4H, *H*<sub>Ar</sub>), 7.48 (m, 3H, *H*<sub>Ar</sub>), 7.35 (m, 3H, *H*<sub>Ar</sub>), 5.84 (s, 2H, N-CH<sub>2</sub>), 3.97 (s, 3H, N-CH<sub>3</sub>). <sup>13</sup>C NMR (DMSO-*d*<sub>6</sub>, 100 MHz): δ 147.04 (C=Se), 141.12 (C<sub>trz</sub>-Ar), 134.28 (C<sub>Ar</sub>), 130.16 (C<sub>Ar</sub>), 130.02 (C<sub>Ar</sub>), 129.40 (C<sub>Ar</sub>), 128.92 (C<sub>Ar</sub>), 128.83 (C<sub>Ar</sub>), 128.70 (C<sub>Ar</sub>), 126.15 (C<sub>Ar</sub>), 53.42 (N-CH<sub>2</sub>), 38.21 (N-CH<sub>3</sub>). FT-IR (neat,  $\bar{\nu}$ ): 3034(w), 2931(w), 1600(w), 1524(w), 1470(w), 1416(m), 1367(m), 1310(s), 1246(m), 1213(w), 1160(s) (C=Se), 1069(s), 1018(m), 838(m), 761(m), 729(m), 690(s), 576(s) cm<sup>-1</sup>.

#### Synthesis of [(**L**<sup>1</sup>)Zn(Cl)<sub>2</sub>(HOMe)] (**1**)

**L**<sup>1</sup> (0.12 g, 0.34 mmol) was added to a solution of ZnCl<sub>2</sub> (0.05 g, 0.33 mmol) in toluene under an argon atmosphere at ambient temperature. Subsequently, the reaction mixture was stirred at 100 °C for 24 h to give a colourless precipitate. The solvent was decanted, and the solid residue was washed with hexane (2 × 5 mL) and dried under a high vacuum. The resulting powder was dissolved in a chloroform and methanol mixture (1:1 ratio). Colourless crystals of **1** were obtained at room temperature. Yield: 80% (based on ZnCl<sub>2</sub>). M.p.: 200–205 °C (decomposed). <sup>1</sup>H NMR (DMSO-*d*<sub>6</sub>, 400 MHz): δ 7.91 (d, *J* = 7.28 Hz, 2H, *H*<sub>Ar</sub>), 7.56 (m, 3H, *H*<sub>Ar</sub>), 7.09 (s, 2H, *H*<sub>Mes</sub>), 4.19 (s, 3H, N-CH<sub>3</sub>), 3.17 (d, 3H, OCH<sub>3</sub>), 2.34 (s, 3H, Ar-CH<sub>3</sub>), 1.98 (s, 6H, Ar-CH<sub>3</sub>). <sup>13</sup>C NMR (DMSO-*d*<sub>6</sub>, 100 MHz): δ 146.65 (C=Se), 140.38 (C<sub>trz</sub>-Mes), 139.85 (C<sub>trz</sub>-Ph), 135.07 (C<sub>Ar</sub>), 132.75 (C<sub>Ar</sub>), 130.11 (C<sub>Ar</sub>), 129.70 (C<sub>Ar</sub>), 128.68 (C<sub>Ar</sub>), 128.37 (C<sub>Ar</sub>), 126.19 (C<sub>Ar</sub>), 48.59 (N-CH<sub>3</sub>), 38.91 (OCH<sub>3</sub>), 20.71 (Ar-CH<sub>3</sub>), 17.41 (Ar-CH<sub>3</sub>). FT-IR (neat,  $\bar{\nu}$ ): 3300(m), 2920(s), 2853(m), 2512(w), 1608(s), 1541(w), 1446(s), 1377(m), 1320(w), 1285(m), 1196(s) (C=Se), 1122(w), 1072(m), 1001(s), 857(s), 778(s), 694(s), 546(m) cm<sup>-1</sup>.

### Synthesis of $[(L^1)Zn(Br)(\mu^2-Br)]_2$ (**2**)

**2** was prepared by a procedure analogous to that of **1**, starting from **L**<sup>1</sup> (0.11 g, 0.30 mmol) and ZnBr<sub>2</sub> (0.07 g, 0.29 mmol). Yield: 74% (based on ZnBr<sub>2</sub>). M.p.: 200–205 °C (decomposed). <sup>1</sup>H NMR (DMSO-*d*<sub>6</sub>, 400 MHz):  $\delta$  7.90 (d, *J* = 6.32 Hz, 2H, *H*<sub>Ar</sub>), 7.57 (m, 3H, *H*<sub>Ar</sub>), 7.09 (s, 2H, *H*<sub>Mes</sub>), 4.20 (s, 3H, N-CH<sub>3</sub>), 2.34 (s, 3H, Ar-CH<sub>3</sub>), 1.98 (s, 6H, Ar-CH<sub>3</sub>). <sup>13</sup>C NMR (DMSO-*d*<sub>6</sub>, 100 MHz):  $\delta$  147.34 (C=Se), 140.17 (C<sub>trz</sub>-Mes), 139.77 (C<sub>trz</sub>-Ph), 135.07 (C<sub>Ar</sub>), 132.85 (C<sub>Ar</sub>), 130.09 (C<sub>Ar</sub>), 129.61 (C<sub>Ar</sub>), 128.63 (C<sub>Ar</sub>), 128.32 (C<sub>Ar</sub>), 126.35 (C<sub>Ar</sub>), 48.56 (N-CH<sub>3</sub>), 20.66 (Ar-CH<sub>3</sub>), 17.39 (Ar-CH<sub>3</sub>). FT-IR (neat,  $\bar{\nu}$ ): 3374(s), 2319(w), 1611(s), 1472(m), 1378(w), 1320(w), 1284(m), 1194(m) (C=Se), 1122(w), 1071(w), 1016(w), 851(m), 686(s) cm<sup>-1</sup>.

### Synthesis of $[(L^2)Zn(Cl)_2(HOMe)]$ (**3**)

**3** was prepared by a procedure analogous to that of **1**, starting from **L**<sup>2</sup> (0.11 g, 0.35 mmol) and ZnCl<sub>2</sub> (0.05 g, 0.35 mmol). Yield: 70% (based on ZnCl<sub>2</sub>). M.p.: 210–215 °C (dec.). <sup>1</sup>H NMR (DMSO-*d*<sub>6</sub>, 400 MHz):  $\delta$  7.90 (d, *J* = 7.04 Hz, 2H, *H*<sub>Ar</sub>), 7.56 (m, 3H, *H*<sub>Ar</sub>), 7.07 (s, 2H, *H*<sub>Mes</sub>), 4.15 (s, 3H, NCH<sub>3</sub>), 2.32 (s, 3H, ArCH<sub>3</sub>), 1.99 (s, 6H, ArCH<sub>3</sub>). <sup>13</sup>C NMR (DMSO-*d*<sub>6</sub>, 100 MHz):  $\delta$  157.00 (C=S), 139.76 (C<sub>trz</sub>-Mes), 136.02 (C<sub>trz</sub>-Ph), 135.32 (C<sub>Ar</sub>), 131.97 (C<sub>Ar</sub>), 129.71 (C<sub>Ar</sub>), 129.36 (C<sub>Ar</sub>), 128.66 (C<sub>Ar</sub>), 128.37 (C<sub>Ar</sub>), 126.26 (C<sub>Ar</sub>), 48.59 (NCH<sub>3</sub>), 20.68 (ArCH<sub>3</sub>), 17.31 (ArCH<sub>3</sub>). FT-IR (neat,  $\bar{\nu}$ ): 3319(s), 1615(s), 1541(w), 1442(s), 1368(m), 1326(s), 1289(s), 1203(s), 1126(m) (C=S), 1071(m), 1001(s), 860(s), 790(w), 753(w), 692(s), 545(s) cm<sup>-1</sup>.

### Synthesis of $[(L^2)Zn(Br)_2(HOMe)]$ (**4**)

**4** was prepared by a procedure analogous to that of **1**, starting from **L**<sup>2</sup> (0.11 g, 0.34 mmol) and ZnBr<sub>2</sub> (0.08 g, 0.33 mmol). Yield: 73% (based on ZnBr<sub>2</sub>). M.p.: 215–220 °C (decomposed). <sup>1</sup>H NMR (DMSO-*d*<sub>6</sub>, 400 MHz):  $\delta$  7.96 (d, *J* = 7.02 Hz, 2H, *H*<sub>Ar</sub>), 7.60 (m, 3H, *H*<sub>Ar</sub>), 7.13 (s, 2H, *H*<sub>Mes</sub>), 4.21 (s, 3H, N-CH<sub>3</sub>), 3.21 (d, 3H, OCH<sub>3</sub>), 2.38 (s, 3H, Ar-CH<sub>3</sub>), 2.05 (s, 6H, Ar-CH<sub>3</sub>). <sup>13</sup>C NMR (DMSO-*d*<sub>6</sub>, 100 MHz):  $\delta$  157.11 (C=S), 139.74 (C<sub>trz</sub>-Mes), 135.97 (C<sub>trz</sub>-Ph), 135.32 (C<sub>Ar</sub>), 131.99 (C<sub>Ar</sub>), 129.70 (C<sub>Ar</sub>), 129.34 (C<sub>Ar</sub>), 128.66 (C<sub>Ar</sub>), 128.36 (C<sub>Ar</sub>), 126.29 (C<sub>Ar</sub>), 48.58 (N-CH<sub>3</sub>), 39.02 (OCH<sub>3</sub>), 20.69 (Ar-CH<sub>3</sub>), 17.32 (Ar-CH<sub>3</sub>). FT-IR (neat,  $\bar{\nu}$ ): 3363(s), 2195(w), 2120(w), 1610(s), 1473(m), 1365(w), 1328(w), 1289(s), 1194(s) (C=S), 1122(m), 1069(m), 1017(s), 851(s), 688(s), 549(m) cm<sup>-1</sup>.

### Synthesis of $[(L^3)Zn(Br)(\mu^2-Br)]_2$ (**5**)

**L**<sup>3</sup> (0.10 g, 0.31 mmol) was added to a solution of ZnBr<sub>2</sub> (0.07 g, 0.31 mmol) in toluene under an argon atmosphere at ambient temperature. Subsequently, the reaction mixture was stirred at 100 °C for 24 h to give a colourless clear solution. Colourless crystals of **5** were obtained at room temperature. Yield: 77% (based on ZnBr<sub>2</sub>). M.p.: 110–115 °C (decomposed). <sup>1</sup>H NMR (CD<sub>3</sub>CN, 400 MHz):  $\delta$  7.61 (m, 5H, *H*<sub>Ar</sub>), 7.51 (d, *J* = 5.82 Hz, 2H, *H*<sub>Ar</sub>), 7.44 (m, 3H, *H*<sub>Ar</sub>), 7.23 (d, *J* = 6.40 Hz, 2H, *H*<sub>Ar</sub>), 5.86 (s, 2H, N-CH<sub>2</sub>), 4.15 (s, 3H, N-CH<sub>3</sub>). <sup>13</sup>C NMR (CD<sub>3</sub>CN, 100 MHz):  $\delta$  145.47 (C=Se), 138.90 (C<sub>trz</sub>-Ar), 136.47 (C<sub>Ar</sub>), 134.43 (C<sub>Ar</sub>), 131.88 (C<sub>Ar</sub>), 131.66 (C<sub>Ar</sub>), 131.50 (C<sub>Ar</sub>), 130.01 (C<sub>Ar</sub>), 129.92 (C<sub>Ar</sub>),

129.83 (C<sub>Ar</sub>), 129.22 (C<sub>Ar</sub>), 126.26 (C<sub>Ar</sub>), 125.78 (C<sub>Ar</sub>), 118.35 (C<sub>Ar</sub>), 56.12 (N-CH<sub>2</sub>), 39.55 (N-CH<sub>3</sub>). FT-IR (neat,  $\bar{\nu}$ ): 3354(s), 2332(w), 2198(w), 2102(w), 2008(w), 1611(s), 1486(m), 1444(m), 1314(s), 1250(m), 1160(m) (C=Se), 1081(s), 1018(s), 807(m), 759(m), 694(s), 639(m), 568(s), 528(m) cm<sup>-1</sup>.

### 1–5 catalysed C–S cross-coupling reactions

The catalytic reactions were performed using a standard Schleck technique using zinc complexes **1–5** as catalysts for the C–S bond coupling reactions of aryl halides and thiols as reported.<sup>39,46</sup> A dry Schlenk tube was charged with 1-bromo-4-nitro benzene (0.20 g, 1 mmol) and thiophenol (0.1 g, 1 mmol), *l*-proline (10 mol%, 0.005 g), and NaO<sup>t</sup>Bu (0.09 g, 0.10 mmol) in CH<sub>3</sub>CN (3 mL). The Schlenk was heated in an oil bath at 80 °C for 15 h. The reaction mixture was then cooled and extracted with ethyl acetate (3 × 15 mL), and the ethyl acetate layer was washed with a saturated aqueous NaCl solution. The organic layer was dried over anhydrous Na<sub>2</sub>SO<sub>4</sub>, and the solvent was removed under reduced pressure in a rotary evaporator. The crude residue was purified by column chromatography using EtOAc–hexane as the eluent to obtain the product as a yellow solid.

## Conclusion

In summary, the first mesoionic heavier chalcogenones, **L**<sup>1</sup>–**L**<sup>3</sup>, were synthesized and characterized. The  $\sigma$  donor and  $\pi$  accepting nature of the mesoionic chalcogenones were investigated using density functional theory. Compared to mesoionic triazolylidene, mesoionic heavier chalcogenones are likely to become a good  $\sigma$ -donor and  $\pi$ -acceptor ligand. Utilizing these ligands, five monomeric and dimeric zinc complexes were prepared in good yields. Compounds **1–5** were characterized in solution by NMR and UV-vis spectroscopy as well as in the solid-state by TGA, FTIR, and single-crystal X-ray diffraction. The UV-vis absorption, thermal, and structural properties of the zinc complexes were significantly influenced by varying the N-substituents of the mesoionic ligands. Single crystal X-ray studies show that the zinc(II) centers in **1–5** are four-coordinated and exhibit distorted tetrahedral geometry. Subsequently, the catalytic application of **1–5** in cross-coupling reactions between thiophenols and aryl halides was demonstrated. **1–5** were active towards C–S bond formation reactions under mild reaction conditions, and this reveals the potential of easily accessible mesoionic chalcogenone Zn(II) compounds in catalysis. Notably, mononuclear zinc(II) complex **1** was more active than **2–5**. The introduction of the heavier chalcogenone ligand in the zinc(II) salt led to increasing catalytic activity, presumably due to its optimized steric and electronic support with the metal center. This strategy contrasts with the previous use of highly reactive diethyl zinc under an inert atmosphere. The present catalysts may thus render a cheap yet effective alternative for expensive late transition metal catalysts in addition to a broad substrate scope.

## Conflicts of interest

There are no conflicts to declare.

## Acknowledgements

We gratefully acknowledge the DST-SERB (EMR/2017/001211) for financial support. VM thanks UGC for the fellowship. VK thanks DST-WOS-A (WOS-A/CS-65/2016) for the fellowship.

## References

- 1 E. Aldeco-Perez, A. J. Rosenthal, B. Donnadiu, B. P. Parameswaran, G. Frenking and G. Bertrand, *Science*, 2009, **236**, 556–559.
- 2 P. L. Arnold and S. Pearson, *Coord. Chem. Rev.*, 2007, **251**, 596–609.
- 3 M. Albrecht, *Chem. Commun.*, 2008, 3601–3610.
- 4 (a) D. Schweinfurth, L. Hettmanczyk, L. Suntrup and B. Sarkar, *Z. Anorg. Allg. Chem.*, 2017, **643**, 554–584; (b) O. Schuster, L. Yang, H. G. Raubenheimer and M. Albrecht, *Chem. Rev.*, 2009, **109**, 3445–3478.
- 5 J. M. Aizpurua, M. Sagartzazu-Aizpurua and Z. Monasterio, *Top. Heterocycl. Chem.*, Springer-Verlag, Berlin Heidelberg, 2015, vol. 40, pp. 211–268.
- 6 R. H. Crabtree, *Coord. Chem. Rev.*, 2013, **257**, 755–766.
- 7 K. O. Marichev, S. A. Patil and A. Bugarin, *Tetrahedron*, 2018, **74**, 2523–2546.
- 8 Á. Vivancos, C. Segarra and M. Albrecht, *Chem. Rev.*, 2018, **118**, 9493–9586.
- 9 G. G. Barrios, M. Soleilhavoup and G. Bertrand, *Acc. Chem. Res.*, 2018, **51**, 3236–3244.
- 10 S. Gründemann, A. Kovacevic, M. Albrecht, J. F. Faller and R. H. Crabtree, *Chem. Commun.*, 2001, 2274–2275.
- 11 M. Begtrup, *J. Chem. Soc., Chem. Commun.*, 1975, 334–335.
- 12 D. Enders, K. Breuer, G. Raabe, J. Runsink, J. H. Teles, J. P. Melder, K. Ebel and S. Brode, *Angew. Chem., Int. Ed. Engl.*, 1995, **34**, 1021–1023.
- 13 P. Mathew, A. Neels and M. Albrecht, *J. Am. Chem. Soc.*, 2008, **130**, 13534–13535.
- 14 G. Guisado-Barrios, J. Bouffard, B. Donnadiu and G. Bertrand, *Angew. Chem., Int. Ed.*, 2010, **49**, 4759–4762.
- 15 K. F. Donnelly, A. Petronilho and M. Albrecht, *Chem. Commun.*, 2013, **49**, 1145–1159.
- 16 (a) A. Petronilho, H. Müller-Bunz and M. Albrecht, *Chem. Commun.*, 2012, **48**, 6499–6501; (b) T. Nakamura, T. Terashima, K. Ogata and S.-I. Fukuzawa, *Org. Lett.*, 2011, **134**, 620–623; (c) S. Hohloch, C.-Y. Su and B. Sarkar, *Eur. J. Inorg. Chem.*, 2011, 3067–3075.
- 17 (a) W.-G. Jia, Y.-B. Huang, Y.-J. Lin and G.-X. Jin, *Dalton Trans.*, 2008, 5612–5620; (b) N. Ghavale, S. T. Manjare, H. B. Singh and R. J. Butcher, *Dalton Trans.*, 2015, **44**, 11893–11900.
- 18 (a) G. K. Rao, A. Kumar, J. Ahmed and A. K. Singh, *Chem. Commun.*, 2010, **46**, 5954–5956; (b) L.-M. Zhang, H.-Y. Li, H.-X. Li, D. J. Young, Y. Wang and J.-P. Lang, *Inorg. Chem.*, 2017, **56**, 11230–11243.
- 19 J. Jin, H.-W. Shin, J. H. Park, J. H. Park, E. Kim, T. K. Ahn, D. H. Ryu and S. U. Son, *Organometallics*, 2013, **32**, 3954–3959.
- 20 H. R. Kim, I. G. Jung, K. Yoo, K. Jang, E. S. Lee, J. Yun and S. U. Son, *Chem. Commun.*, 2010, **46**, 758–760.
- 21 K. Srinivas, C. N. Babu and G. Prabusankar, *Dalton Trans.*, 2015, **44**, 15636–15644.
- 22 E. Alvarado, A. C. Badaj, T. G. Larocque and G. G. Lavoie, *Chem. – Eur. J.*, 2012, **18**, 12112–12121.
- 23 K. Srinivas and G. Prabusankar, *Dalton Trans.*, 2017, **46**, 16615–16622.
- 24 K. Srinivas and G. Prabusankar, *RSC Adv.*, 2018, **8**, 32269–32282.
- 25 H.-N. Zhang, W.-G. Jia, Q.-T. Xu and C.-C. Ji, *Inorg. Chim. Acta*, 2016, **450**, 315–320.
- 26 C. N. Babu, K. Srinivas and G. Prabusankar, *Dalton Trans.*, 2016, **45**, 6456–6465.
- 27 K. Srinivas, P. Suresh, C. N. Babu, A. Sathyanarayana and G. Prabusankar, *RSC Adv.*, 2015, **5**, 15579–15590.
- 28 K. Srinivas, A. Sathyanarayana, C. N. Babu and G. Prabusankar, *Dalton Trans.*, 2016, **45**, 5196–5209.
- 29 Y.-B. Huang, W.-G. Jia and G.-X. Jin, *J. Organomet. Chem.*, 2009, **694**, 86–90.
- 30 A. K. Sharma, H. Joshi, R. Bhaskar and A. K. Singh, *Dalton Trans.*, 2017, **46**, 2228–2237.
- 31 O. Prakash, K. N. Sharma, H. Joshi, P. L. Gupta and A. K. Singh, *Organometallics*, 2014, **33**, 2535–2543.
- 32 A. K. Sharma, H. Joshi, K. N. Sharma, P. L. Gupta and A. K. Singh, *Organometallics*, 2014, **33**, 3629–3639.
- 33 P. Dubey, S. Gupta and A. K. Singh, *Dalton Trans.*, 2018, **47**, 3764–3774.
- 34 M. Vaddamanu, R. Karupnaswamy, K. Srinivas and G. Prabusankar, *ChemistrySelect*, 2016, **1**, 4668–4671.
- 35 A. Sathyanarayana, K. Srinivas, A. Mandal, S. Gharami and G. Prabusankar, *J. Chem. Sci.*, 2014, **126**, 1589–1595.
- 36 D. J. Williams, K. M. White, D. VanDerveer and A. P. Wilkinson, *Inorg. Chem. Commun.*, 2002, **5**, 124–126.
- 37 U. Flörke, A. Ahmida, H. Egold and G. Henkel, *Acta Crystallogr.*, 2014, **E70**, m384.
- 38 (a) A. Ghaderi, *Tetrahedron*, 2016, **72**, 4758–4782; (b) L. Guo and M. Rueping, *Acc. Chem. Res.*, 2018, **51**, 1185–1195.
- 39 For selected examples: (a) C.-F. Lee, Y.-C. Liu and S. S. Badsara, *Chem. – Asian J.*, 2014, **9**, 706–722 and references there in; (b) P. Shaw, A. R. Kennedy and D. J. Nelson, *Dalton Trans.*, 2016, **45**, 11772–11780; (c) L.-H. Zou, C. Zhao, P.-G. Li, Y. Wang and J. Li, *J. Org. Chem.*, 2017, **82**, 12892–12898; (d) V. Ritleng, M. Henrion and M. J. Chetcuti, *ACS Catal.*, 2016, **6**, 890–906; (e) K. D. Jones, D. J. Power, D. Bierer, K. M. Gericke and S. G. Stewart, *Org. Lett.*, 2018, **20**, 208–211; (f) K. Choudhuri, S. Maiti and P. Mal, *Adv. Synth. Catal.*, 2019, **361**, 1092–1101; (g) P. H. Gehrtz, V. Geiger, T. Schmidt, L. Sršan and I. Fleischer, *Org. Lett.*, 2018, **21**, 50–55; (h) N. Hazari, P. R. Melvin and M. M. Beromi, *Nat. Rev. Chem.*, 2017, **1**, 0025; (i) C.-W. Chen, Y.-L. Chen, D. M. Reddy, K. Du, C.-E. Li, B.-H. Shih, Y.-J. Xue and

- C.-F. Lee, *Chem. – Eur. J.*, 2017, **23**, 10087–10091; (j) J. L. Farmer, M. Pompeo, A. J. Lough and M. G. Organ, *Chem. – Eur. J.*, 2014, **20**, 15790–15798; (k) C. C. Eichman and J. P. Stambuli, *Molecules*, 2011, **16**, 590–608.
- 40 M. Kosugi, T. Shimizu and T. Migita, *Chem. Lett.*, 1978, 13–14.
- 41 G. T. Venkanna, H. D. Arman and Z. J. Tonzetich, *ACS Catal.*, 2014, **4**, 2941–2950.
- 42 X. Liu, S.-B. Zhang, H. Zhu and Z.-B. Dong, *J. Org. Chem.*, 2018, **83**, 11703–11711.
- 43 S.-C. Lee, H.-H. Liao, A. Chatupheeraphat and M. Rueping, *Chem. – Eur. J.*, 2018, **24**, 3608–3612.
- 44 B. Liu, C.-H. Lim and G. M. Miyake, *J. Am. Chem. Soc.*, 2017, **139**, 13616–13619.
- 45 M. S. Oderinde, M. Frenette, D. W. Robbins, B. Aquila and J. W. Johannes, *J. Am. Chem. Soc.*, 2016, **138**, 1760–1763.
- 46 A. P. Thankachan, K. S. Sindhu, K. K. Krishnan and G. Anilkumar, *RSC Adv.*, 2015, **5**, 32675–32678.
- 47 M. A. B. Azam and B. Suresh, *Sci. Pharm.*, 2012, **80**, 789–823.
- 48 X. Liu, S.-B. Zhang, H. Zhu and Z.-B. Dong, *J. Org. Chem.*, 2018, **83**, 11703–11711.
- 49 A. Correa, M. Carril and C. Bolm, *Angew. Chem., Int. Ed.*, 2008, **47**, 2880–2883.
- 50 Y. Liu, B. Huang, X. Cao, D. Wu and J.-P. Wan, *RSC Adv.*, 2014, **4**, 37733–37737.
- 51 G. He, Y. Huang, Y. Tong, J. Zhang, D. Zhao, S. Zhou and S. Han, *Tetrahedron Lett.*, 2013, **54**, 5318–5321.
- 52 P. R. Christensen and M. O. Wolf, *Adv. Funct. Mater.*, 2016, **26**, 8471–8477.
- 53 (a) B. Liu, C.-H. Lim and G. M. Miyake, *J. Am. Chem. Soc.*, 2017, **139**, 13616–13619; (b) D. A. Boyd, *Angew. Chem., Int. Ed.*, 2016, **55**, 15486–15502; (c) E. A. Ilardi, E. Vitaku and J. T. Njardarson, *J. Med. Chem.*, 2014, **57**, 2832–2842; (d) M. Feng, B. Tang, S. Liang and X. Jiang, *Curr. Top. Med. Chem.*, 2016, **16**, 1200–1216; (e) G. A. Patani and E. J. LaVoie, *Chem. Rev.*, 1996, **96**, 3147–3176.
- 54 For example: (a) X. Gao, J. L. Hodgson, D. Jiang, S. B. Zhang, S. Nagase, G. P. Miller and Z. Chen, *Org. Lett.*, 2011, **13**, 3316–3319; (b) P. R. Christensen, B. O. Patrick, É. Caron and M. O. Wolf, *Angew. Chem., Int. Ed.*, 2013, **52**, 12946–12950.
- 55 T. Scattolin, E. Senol, G. Yin, Q. Guo and F. Schoenebeck, *Angew. Chem., Int. Ed.*, 2018, **57**, 12425–12429.
- 56 O. V. Dolomanov, L. J. Bourhis, R. J. Gildea, J. A. K. Howard and H. Puschmann, *J. Appl. Crystallogr.*, 2009, **42**, 339–341.
- 57 L. J. Bourhis, O. V. Dolomanov, R. J. Gildea, J. A. K. Howard and H. Puschmann, *Acta Crystallogr.*, 2015, **A71**, 59–75.
- 58 L. J. Bourhis, O. V. Dolomanov, R. J. Gildea, J. A. K. Howard and H. Puschmann, *Acta Crystallogr.*, 2015, **A71**, 59–75.